Knockdown of GSG2 inhibits prostate cancer progression *in vitro* and *in vivo*

FENG YU[1], YUANYUAN LIN[2], XINPING XU[3], WEIPENG LIU[4], DAN TANG[5],
XIAOCHEN ZHOU[4], GONGXIAN WANG[4], YI ZHENG[6] and AN XIE[7]

[1]Department of Oncology, The First Affiliated Hospital of Nanchang University; [2]Department of Hematology,
Jiangxi Provincial Children's Hospital; [3]Jiangxi Institute of Respiratory Disease; [4]Department of Urology;
[5]Department of Geriatrics, The First Affiliated Hospital of Nanchang University, Nanchang, Jiangxi 330006;
[6]Department of Urology, The Second Affiliated Hospital of Zhejiang University, Hangzhou, Zhejiang 310009;
[7]Jiangxi Institute of Urology, The First Affiliated Hospital of Nanchang University, Nanchang, Jiangxi 330006, P.R. China

Abstract. Prostate cancer (PCa) is the second leading cause of cancer-related death among men worldwide. The present study aimed to investigate the role of germ cell-specific gene 2 protein (GSG2), also termed histone H3 phosphorylated by GSG2 at threonine-3, in the development and progression of PCa. GSG2 expression levels in PCa tissues and para-carcinoma tissues was detected by immunohistochemistry. The GSG2 knockdown cell model was constructed by lentivirus infection, and the knockdown efficiency was verified by qPCR and WB. In addition, the effects of shGSG2 on cell proliferation, colony formation and apoptosis were evaluated by Celigo cell counting assay, Giemsa staining and flow cytometry, respectively. Tumor development in nude mice was also detected. GSG2 expression was upregulated in PCa tissues and human PCa cell lines PC-3 and DU 145. High expression of GSG2 in tumor samples was associated with progressed tumors. GSG2 knockdown suppressed cell proliferation and colony formation, but promoted apoptosis, which was also verified *in vivo*. The results of the present study revealed that GSG2 upregulation was associated with PCa progression; GSG2 knockdown inhibited cell proliferation and colony formation and induced apoptosis, and may therefore serve as a potential therapeutic target for PCa therapy.

Correspondence to: Dr An Xie, Jiangxi Institute of Urology, The First Affiliated Hospital of Nanchang University, 17 Yongwaizheng Street, Nanchang, Jiangxi 330006, P.R. China
E-mail: xiean123kxy@163.com

Abbreviations: PCa, prostate cancer; GSG2, germ cell-specific gene 2 protein; ePK, eukaryotic protein kinase; H3T3ph, histone H3 phosphorylated by GSG2 at threonine-3; ADT, androgen deprivation therapy; FACS, fluorescence-activated cell sorting; shRNA, short hairpin RNA; shGSG2, cells transfected with GSG2-targeting shRNA; shCtrl, cells transfected with control shRNA

Introduction

Prostate cancer (PCa) is one of the most common malignant tumors of the male genitourinary system and the second leading cause of death among men worldwide (1). There were 1,276,106 new cases and 358,989 deaths (3.8% of all deaths caused by cancer in men) associated with PCa in 2018 (2). Risk factors for PCa include age, ethnicity, family history and diet; among those, age is the most consistent factor (3). The incidence of PCa is highest among older men, with millions of people suffering from this disease (4,5). Lifestyle modifications such as smoking cessation, exercise and weight control may help to decrease the risk of PCa (6). Primary PCa is curable; in addition to the combination of surgery and multiagent chemotherapy, androgen deprivation therapy (ADT) has been used as the first-line treatment for PCa (7,8). Although ADT is usually initially effective, the improvement in the prognosis of PCa is still far from satisfying (9). Since therapeutic agents act by natural selection to promote the acquisition of new tumor traits, PCa becomes resistant to ADT, resulting in a fatal outcome known as castration-resistant PCa (CRPC) (10). In addition, recurrent and metastatic PCa is typically lethal (11). Along with the development of molecular medicine, various potential key factors in the development of PCa have been identified. For example, GALNT7 and ST6GalNAc1 have been reported to be significantly upregulated in clinical PCa tissues (9). Despite such advances, more accurate and specific targets still need to be explored to benefit patients with PCa.

Germ cell-specific gene 2 (GSG2), also termed haploid germ cell-specific nuclear protein kinase, is an atypical serine/threonine-protein kinase that is present in all major eukaryotic phyla, including yeasts, microsporidia, plants, nematodes, flies, fish, amphibians and mammals (12). GSG2 has long been considered an inactive pseudokinase due to its low structural homology with classical protein kinases (13). However, GSG2 is responsible for the phosphorylation of

histones, particularly histone H3 at Thr3 (H3T3) during mitosis, which serves a role in chromosome segregation and thus has a great potential as an anticancer therapeutic target (14). In addition, phosphorylation of H3T3 by GSG2 creates a recognition motif for docking of the chromosomal passenger complex, which is essential for the progression of cell division (15). GSG2 overexpression has been demonstrated to serve an important role in cancer cells, where it interrupts the normal dissociation of centromeric cohesion (16), which leads to a delay before metaphase and ultimately results in defective mitosis (17). Han *et al* (18) have reported that GSG2 may be considered as a viable anti-melanoma target, and the concomitant inhibition of GSG2 may represent a novel therapeutic strategy with improved efficacy for the treatment of melanoma. Nevertheless, the role of GSG2 in PCa has not been reported to the best of our knowledge and remains largely unclear. Therefore, the present aimed to demonstrate for the first time the expression of GSG2 in PCa and its role in the development and progression of PCa, and to determine the role that GSG2 may serve in the treatment and prognosis of PCa as a potential therapeutic target.

Materials and methods

Materials. DU 145 (HTB-81) and PC-3 (CRL-1435) cell lines were purchased from the Cell Bank of the Chinese Academy of Sciences and cultured with 90% RPMI-1640 (Sigma-Aldrich; Merck KGaA) and 10% FBS (Gibco; Thermo Fisher Scientific, Inc.) medium at 37°C in a humidified incubator containing 5% CO_2. TOP10 *Escherichia coli* competent cells (CB104-03) purchased from Tiangen Biotech Co., Ltd. were cultured with Luria-Bertani (LB) liquid medium (1% tryptone, 0.5% yeast extract and 1% NaCl) at 37°C with gentle agitation. Anti-GSG2 (cat. no. ab21686; Abcam), anti-GAPDH (cat. no. AP0063; Bioworld Technology, Inc.) and anti-Ki67 (cat. no. ab16667; Abcam) primary antibodies, HRP-conjugated goat anti-rabbit IgG (cat. no. A0208; Beyotime Institute of Biotechnology) for western blotting, HRP-conjugated goat anti-rabbit IgG (cat. no. ab6721; Abcam) for immunohistochemical staining and western blotting.

Female BALB/c nude mice (4-week old) were purchased from Shanghai SLAC Laboratory Animal Co. Ltd. and divided into two groups randomly (n=6 mice/group). All mice were housed under standard housing conditions as previously described (19).

PCa and normal prostate tissues (>5 cm away from the PCa tissue) were collected from patients (mean age, 59 years) who had been diagnosed with PCa and underwent surgical resection in the First Affiliated Hospital of Nanchang University (Nanchang, China) between May 2015 and May 2017, and the age range of patients was between 20 and 97 years. Ethical approval was obtained from the Ethics Committee of the First Affiliated Hospital of Nanchang University, and written informed consent was obtained from all patients.

Immunohistochemical staining. PCa and normal prostate tissues from 159 patients were collected, and the expression of GSG2 in PCa and normal prostate tissues was detected by immunohistochemistry. Following dewaxing of the paraffin-embedded sections, antigen retrieval was performed with citrate buffer,

followed by incubation with 3% H_2O_2 at room temperature for 10 min. The paraffin sections were incubated with the primary antibody against GSG2 (1:200) at 4°C overnight and subsequently incubated with the secondary antibody (1:400) at room temperature for 30 min. Paraffin sections were stained with 3-3' diaminobenzidine (DAB) at room temperature for 10 min and counterstained with hematoxylin at room temperature for 2 min. For each section, 10 fields (x100 magnification) were selected to be captured using an Olympus optical microscope (Olympus Corporation) and analyzed. The scoring standard for GSG2 staining intensity was graded as 0 (negative), 1 (weak), 2 (positive ++) and 3 (positive +++). The staining extent was graded as 0 (0%), 1 (1-25%), 2 (26-50%), 3 (51-75%) or 4 (76-100%). The staining intensity varied from weak to strong. The sections were classified into negative (0 points), positive (1-4 points), ++ positive (5-8 points) or +++ positive (9-12 points) based on the sum of the staining intensity and staining extent scores. If the score of the sections was above the median, the expression of GSG2 was high; if the score was below the median, the expression of GSG2 was low.

Target gene RNA interference lentiviral vector preparation. The GSG2 gene was used as a template to design an RNA interference target sequence (target sequence 5'-CCACAGGACAATGCTGAACTT-3') to synthesize a single-stranded DNA oligo, which was then paired to generate double-stranded DNA. The negative control interference target sequence was 5'-TTCTCCGAACGTGTCACGT-3'. Subsequently, the double-stranded DNA was directly ligated into the double-digested linearized BR-V-108 lentivirus vector (Shanghai Yibeirui Biomedical Science and Technology Co., Ltd) overnight. The ligation product was transferred to TOP10 *E. coli* competent cells (TIANGEN) with antibiotic-free LB liquid medium and incubated at 37°C for 1 h. The correctly cloned bacterial solution was screened by bacterial liquid PCR amplification and sequencing for plasmid extraction. Bacterial liquid PCR amplification was performed using a Taq Plus Master Mix (Vazyme Biotech Co., ltd.), forward and reverse primers (GeneRay Biotech Co., Ltd.), a single TOP10 *E. coli* cell colony and ddH$_2$O. The reaction conditions were as follows: 94°C for 3 min, 42 cycles of 94°C for 30 sec, 55°C for 30 sec and 72°C for 30 sec, and a final extension at 72°C for 5 min. The quality-eligible plasmids were used for lentiviral packaging. The primer sequences were as follows: Negative control interference target forward, 5'-CCATGATTCCTT CATATTTGC-3' and reverse, 5'-GTAATACGGTTATCC ACGCG-3'; GSG2 RNA interference target forward, 5'-CCT ATTTCCCATGATTCCTTCATA-3' and reverse, 5'-GTAATA CGGTTATCCACGCG-3'.

Cell infection and fluorescence immunoassay. DU 145 and PC-3 cells were infected with lentivirus containing GSG2 interference target sequences (1x10^7 TU/ml) or negative control interference target sequences (1x10^7 TU/ml), and the cells were then cultured at 37°C for 72 h. A fluorescent microscope (EMD Millipore) was used to observe the expression of green fluorescent protein (GFP, carried by the lentivirus vector) to assess infection efficiency. The infection efficiency was evaluated by the ratio of fluorescent cells to total cells (observed under white light).

Reverse transcription-quantitative PCR (RT-qPCR). DU 145 and PC-3 cells were collected and centrifuged at 800 x g for 5 min at room temperature. The supernatant was removed, and total RNA was isolated using the TRIzol® reagent (Thermo Fisher Scientific, Inc.) according to the manufacturer's instructions. The M-MLV Reverse Transcriptase kit (Promega Corporation) was used to synthesize cDNAs. The reverse transcription primers, total RNA, M-MLV-RTase and Rnasin were mixed at 42˚C for 1 h and incubated in water at 70˚C for 10 min to inactivate the RT enzyme. The reaction system for qPCR was prepared by real-time quantitative PCR instrument (Applied Biosystems; Thermo Fisher Scientific, Inc.) according to the manufacturer's instructions. The reaction system included: SYBR® Premix Ex Taq (Takara Biotechnology Co., Ltd.), upstream and downstream primers (GeneRay Biotech Co., Ltd.), reverse transcription products and RNase-Free H_2O. The reaction conditions were as follows: 95˚C for 30 sec (predenaturation), 95˚C for 15 sec (denaturation) and 60˚C for 10 sec (annealing) for a total of 42 cycles, and 72˚C for 5 min (elongation). GAPDH was used as the internal reference. The relative expression of genes was calculated using the $2^{-\Delta\Delta Cq}$ method (20). Each experiment was repeated three times. The primer sequences were as follows: GAPDH forward, 5'-TGACTTCAACAG CGACACCCA-3' and reverse, 5'-CACCCTGTTGCTGTA GCCAAA-3'; GSG2 forward, 5'-GGAAGGGGTGTTTGG CGAAGT-3' and reverse, 5'-TGAGGAGCAAGGGAGGGT AAG-3'.

Western blot assay. The expression levels of GSG2 in PCa cell lines and tumor tissues from mice were detected by western blotting. DU 145 and PC-3 cells were collected and lysed with RIPA lysis buffer (Beyotime Institute of Biotechnology) containing protease inhibitors on ice according to the manufacturer's instructions. BCA Protein Assay kit (HyClone; GE Healthcare Life Sciences) was used to detect the concentration of the extracted protein. SDS-PAGE (10%) was performed to isolate the total cellular proteins with 20 μg protein/lane, which were then transferred to PVDF membranes. The membranes were blocked with TBS + 0.1% Tween-20 (TBST) solution containing 5% skimmed milk for 60 min at room temperature and incubated with the primary anti-GSG2 (1:1,000) and anti-GAPDH (1:3,000) antibodies overnight at 4˚C. After washing with TBST, the membranes were incubated with the HRP-conjugated goat anti-rabbit IgG polyclonal antibody (1:3,000) for 2 h at room temperature. Color development for signal detection was performed using the ECL™ Prime Western Blotting Detection Reagent kit (Amersham; GE Healthcare Life Sciences). The experiment was performed in triplicate.

Celigo cell count assay. Short hairpin (sh)RNA lentivirus-infected DU 145 and PC-3 cells at the logarithmic growth phase were trypsinized, resuspended in complete medium (RPMI-1640 + 10% FBS), counted and seeded in 96-well plates (2,000 cells/well). The next day, the plate was detected by Celigo Imaging Cytometry System (Nexcelom Bioscience) to count the cells, which was repeated once a day for 5 consecutive days. This experiment was performed independently three times.

Fluorescence-activated cell sorting (FACS) assay. Apoptosis was determined by FACS assay. Following infection with shRNA lentivirus, DU 145 and PC-3 cells were cultured in 6-well plates until the cell density reached 85%. The cells were trypsinized and centrifuged to collect the cell pellet, which was washed with D-Hank's solution precooled at 4˚C. Cell suspensions (100 μl; $1x10^5$-$1x10^6$ cells) were stained with 5 μl Annexin V-APC (cat. no. 10010-09; Southern Biotech) in the dark at room temperature for 15 min, centrifuged at 1,000 x g at room temperature for 3 min and resuspended. Subsequently, 5 μl propidium iodide (PI) was added to the cell suspension, which was replenished to 300 μl with the cell dye buffer from the apoptosis kit. The cells were detected with a Guava easy-Cyte HT flow cytometer (EMD Millipore) and analyzed by FlowJo VX10 (FlowJo LLC). In the graph of apoptosis results, the lower left quadrant represented living cells and the two right quadrants represented apoptotic cells, of which the upper right quadrant represented late apoptotic cells and the lower right quadrant represented early apoptotic cells. The experiment was performed in triplicate.

Colony formation assay. Three days after shRNA lentivirus infection, DU 145 and PC-3 cells in the logarithmic growth phase were digested with trypsin, resuspended in complete medium and inoculated into 6-well plates (1,000 cells/well). Cells were cultured for additional 8 days, and the medium was changed every 3 days. Subsequently, the cells were fixed with 4% paraformaldehyde at room temperature for 1 h after washing with PBS. Giemsa was used for staining the cells at room temperature for 20 min, and double distilled H_2O was used to wash the cells three times. The cells were dried and images were captured using a digital camera to count the number of colonies containing >50 cells. The assay was performed in triplicate.

Tumor-bearing animal model. All animal experiments were approved and performed under the supervision of the Institutional Animal Care and Use Ethics Committee of the First Affiliated Hospital of Nanchang University. PC-3 cells infected with the shRNA lentivirus at the logarithmic growth phase were digested with trypsin, resuspended and subcutaneously injected into the right forelimb armpit of each nude mouse (200 μl suspension containing $4x10^6$ cells/ml). All mice were maintained for 35 days, during which the volume of tumors in the mice was measured nine times with a Vernier caliper. On day 35, the mice were intraperitoneally injected with D-Luciferin (10 μg) for 15 min, anesthetized by intraperitoneal injection of 0.7% pentobarbital sodium (70 mg/kg) and placed under a small animal multispectral living imaging system for imaging (Lumina LT; PerkinElmer, Inc.). Subsequently, the mice were sacrificed by cervical dislocation, and tumors were dissected from the mice to measure the tumor volume and weight. The formula for the calculation of the tumor volume in mm^3 was as follows: $V=\pi/6 \times L \times W^2$, where V is the tumor volume, L is the tumor length and W is the tumor width. In addition, the expression of GSG2 in tumor tissues from mice in the control (shCtrl) and GSG2-knockdown (shGSG2) groups was detected by western blotting as described above, and the isolated tumors were preserved in liquid nitrogen at -80˚C.

Ki-67 staining. Paraffin sections of tumor tissues removed from mice were dewaxed, rehydrated in a descending ethanol gradient (100, 95, 80 and 70%) and incubated with an anti-Ki-67 antibody (1:200) at 4°C overnight. After washing with PBS, the paraffin sections were incubated with a secondary antibody (1:400) for 2 h at room temperature, and then counterstained with hematoxylin and observed under an Olympus optical microscope (x100 or x200 magnification) to analyze Ki-67 expression. A total of 10 fields were selected for each section to be captured and analyzed. The experiment was performed in triplicate.

Human RTK Phosphorylation Antibody Array. To investigate the potential downstream signaling pathway and functional targets of GSG2 in PC-3 cells, Human RTK Phosphorylation Antibody Array (cat. no. ab193662; Abcam) was used. PC-3 cells infected with shCtrl or shGSG2 were resuspended and lysed with 1X lysis buffer for 30 min. Simultaneously, the membranes were blocked with 2 ml 1X Blocking Buffer for 30 min at room temperature. Subsequently, the samples were pipetted into wells and incubated overnight at 4°C. Following washing, 1 ml 1X biotinylated anti-phosphotyrosine antibody was added to each well and incubated overnight at 4°C. Next, 2 ml 1X HRP-conjugated streptavidin was added into each well and incubated for 2 h at room temperature. After the membranes were washed, any excess washing buffer was removed by blotting the membrane edges, and 500 μl detection buffer mixture (equal volumes of Detection Buffer C and Detection Buffer D) was added to each membrane for 2 min at room temperature. The signal density was detected using a chemiluminescence imaging system and analyzed by ImageJ software version 1.8.0 (National Institutes of Health). The experiment was performed in duplicate.

Statistical analysis. Data were analyzed using GraphPad Prism 6 software (GraphPad Software, Inc.) and presented as the mean ± standard deviation. Unpaired Student's t-test was used to compare the differences between two groups. The differences in GSG2 expression between patients with PCa with different clinicopathological characteristics were compared using the chi-square test. The correlation between GSG2 expression and clinicopathological characteristics was analyzed by Spearman rank correlation analysis. The plot histogram of GSG2-related signaling molecules in cancer cells was produced using SignaLink 2.0 analysis. P<0.05 was considered to indicate a statistically significant difference.

Results

Expression of GSG2 in clinical PCa tissues. To investigate the role of GSG2 in the development and progression of PCa, the expression of GSG2 was detected in clinical PCa and para-carcinoma tissues by immunohistochemical staining. As presented in Fig. 1A, the results indicated a cytoplasmic localization of GSG2 and demonstrated that the expression of GSG2 in PCa tissues was significantly upregulated compared with that in para-carcinoma tissues (Table I). In addition, the association between the expression of GSG2 and the clinicopathological characteristics of patients with PCa was evaluated by statistical analysis. The results indicated

Table I. GSG2 expression patterns in prostate cancer tissues and para-carcinoma tissues determined by immunohistochemistry analysis.

GSG2 expression	Tumor tissue N	%	Para-carcinoma tissue N	%	P-value
Low	93	58.5	80	100	0.000[a]
High	66	41.5	0	0	

[a]P<0.01. GSG2, germ cell-specific gene 2.

significant differences in GSG2 expression levels among patients with different Gleason scores (grade) and pathological grades (P<0.05; Table II). Spearman rank correlation analysis revealed that the Gleason score (grade) and pathological grade were weakly positively correlated with GSG2 expression levels (Table III). These results demonstrated that the gene expression of GSG2 was significantly associated with the development and progression of PCa.

Knockdown of GSG2 in PCa cells. To investigate the role of GSG2 in PCa, shRNA targeting GSG2 was cloned into lentiviral vectors carrying GFP. Subsequently, shGSG2 or shCtrl lentivirus was infected into human PCa cells PC-3 and DU 145. As presented in Fig. 1B, the fluorescence intensity in cells infected with shGSG2 or shCtrl revealed >80% transfection efficiency in the two cell lines. The relative expression levels of GSG2 in PC-3 and DU 145 cells were detected by RT-qPCR; the results demonstrated that the GSG2 mRNA level was reduced by 70.8% in PC-3 cells and by 57.7% in DU 145 cells in the shGSG2 groups compared with the shCtrl groups (P<0.05; Fig. 1C). In addition, western blotting also demonstrated that GSG2 protein expression was significantly downregulated post-infection compared with that in cells infective with shCtrl (Fig. 1D). These results indicated the successful construction of a GSG2-knockdown cell model.

Knockdown of GSG2 inhibits PCa cell proliferation and promotes apoptosis. In order to examine the effects of GSG2 on cell proliferation, Celigo Imaging Cytometry System was used for analysis of the cell growth curve. As presented in Fig. 2A, cell proliferation was significantly inhibited in the shGSG2 group compared with that in the shCtrl group in PC-3 and DU 145 cells. In addition, colony formation assay was performed to assess the colony formation ability of PCa cells, which is an important feature of malignant tumors. The number of cell colonies was significantly decreased by 80.0 and 66.7%, respectively, in the shGSG2 group of PC-3 and DU 145 cells compared with that of the shCtrl group (P<0.05; Fig. 2B). To detect the effects of GSG2 knockdown on the apoptosis of PCa cells, FACS was used. Compared with that of the shCtrl group, the percentage of apoptotic cells in the shGSG2 group was increased 2.5-fold in PC-3 cells and 6-fold in DU 145 cells (P<0.05; Fig. 3), suggesting that GSG2 knockdown promoted the apoptosis of PCa cells.
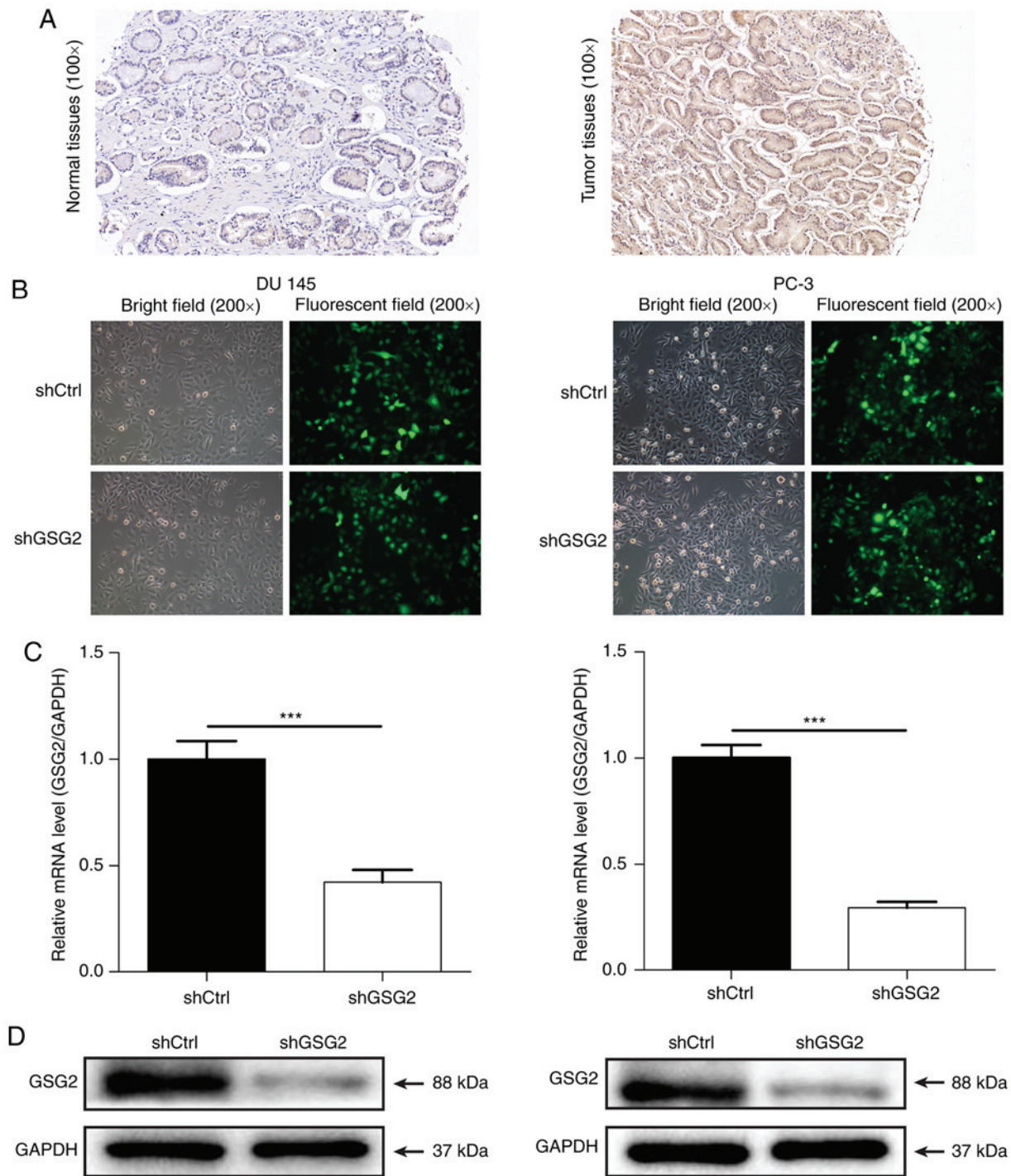
Figure 1. Expression of GSG2 in PCa tissues GSG2 and construction of a GSG2-knockdown cell model. (A) Representative immunohistochemical staining results: Low expression of GSG2 in adjacent normal tissues and high expression of GSG2 in PCa tissues (magnification, x100). (B) Transfection efficiency was examined by fluorescence imaging in PC-3 and DU 145 cells (magnification, x200). (C) GSG2 mRNA expression was determined by reverse transcription-quantitative PCR in PC-3 and DU 145 cells. (D) GSG2 protein expression level was detected by western blotting in PC-3 and DU 145 cells. ***P<0.001. GSG2, germ cell-specific gene 2; PCa, prostate cancer; shGSG2, cells transfected with GSG2-targeting short hairpin RNA; shCtrl, cells transfected with the control short hairpin RNA.

Effects of GSG2 knockdown on tumor progression in vivo. To determine the potential of shGSG2 as a therapeutic target for PCa therapy, a nude mouse xenograft model was constructed using GSG2-knockdown PC-3 cells. At 72 h post-infection of PC-3 cells with shGSG2 or shCtrl lentivirus, the infection efficiency was determined to be 90-100% (Fig. S1), and the mice were subcutaneously injected with these cells. The levels

of bioluminescence intensity (μW/cm^2) were measured by *in vivo* imaging of anaesthetized mice following an injection of D-luciferin. The bioluminescence intensity in the shGSG2 group was ~71% lower compared with that in the shCtrl group (P<0.05; Fig. 4A and B). The results suggested that tumor growth was slower in the shGSG2 group compared with the shCtrl group (P<0.05). In addition, according to the tumor

Table II. Relationship between GSG2 expression levels and clinicopathological characteristics of patients with prostate cancer.

| | No. of patients | | GSG2 expression | | | | |
| | | | Low | | High | | |
Characteristic	N	%	N	%	N	%	P-value
All patients	159		93	58.5	66	41.5	
Age, years							0.184
≤69	84	52.8	45	28.3	39	24.5	
>69	75	47.2	48	30.2	27	17.0	
Gleason Score							0.043[a]
<8	60	37.7	40	25.2	20	12.6	
≥8	92	57.9	46	28.9	46	28.9	
Grade							0.005[b]
1	12	7.5	10	6.3	2	1.3	
2	38	23.9	26	16.4	12	7.5	
3	102	64.2	50	31.4	52	32.7	
T Infiltrate							0.553
T1	2	1.3	2	1.3	0	0.0	
T2	68	42.8	49	30.8	19	11.9	
T3	38	23.9	28	17.6	10	6.3	
T4	6	3.85	6	3.8	0	0.0	
Lymphatic metastasis							0.088
N0	106	66.7	77	48.4	29	18.2	
N1	8	5.0	8	5.0	0	0.0	
Stage							0.833
1	14	8.8	13	8.2	1	0.6	
2	56	35.2	38	23.9	18	11.3	
3	32	20.1	22	13.8	10	6.3	
4	12	7.5	12	7.5	0	0.0	
Gleason grade							0.026[a]
2	8	5.0	6	3.8	2	1.3	
3	38	23.9	28	17.6	10	6.3	
4	54	34.0	26	16.4	28	17.6	
5	51	32.1	25	15.7	26	16.4	
6	1	0.6	1	0.6	0	0.0	

[a]P<0.05, [b]P<0.01. GSG2, germ cell-specific gene 2.

Table III. Correlation between GSG2 expression and tumor characteristics in patients with prostate cancer.

Characteristic	N	Spearman's r	P-value
Gleason score	152	0.164	0.043[a]
Gleason grade	152	0.181	0.025[a]
Grade	152	0.227	0.005[b]

[a]P<0.05, [b]P<0.01. r, correlation coefficient; GSG2, germ cell-specific gene 2.

volume and weight, tumors from mice in the shGSG2 group were 66% smaller in diameter, and the tumor weight was 69% lower compared with those in the shCtrl group (P<0.05; Fig. 4C-E). The expression of GSG2 in tumor tissues from mice was inhibited in the shGSG2 group compared with the shCtrl group (Fig. 4F). Ki-67 staining demonstrated that
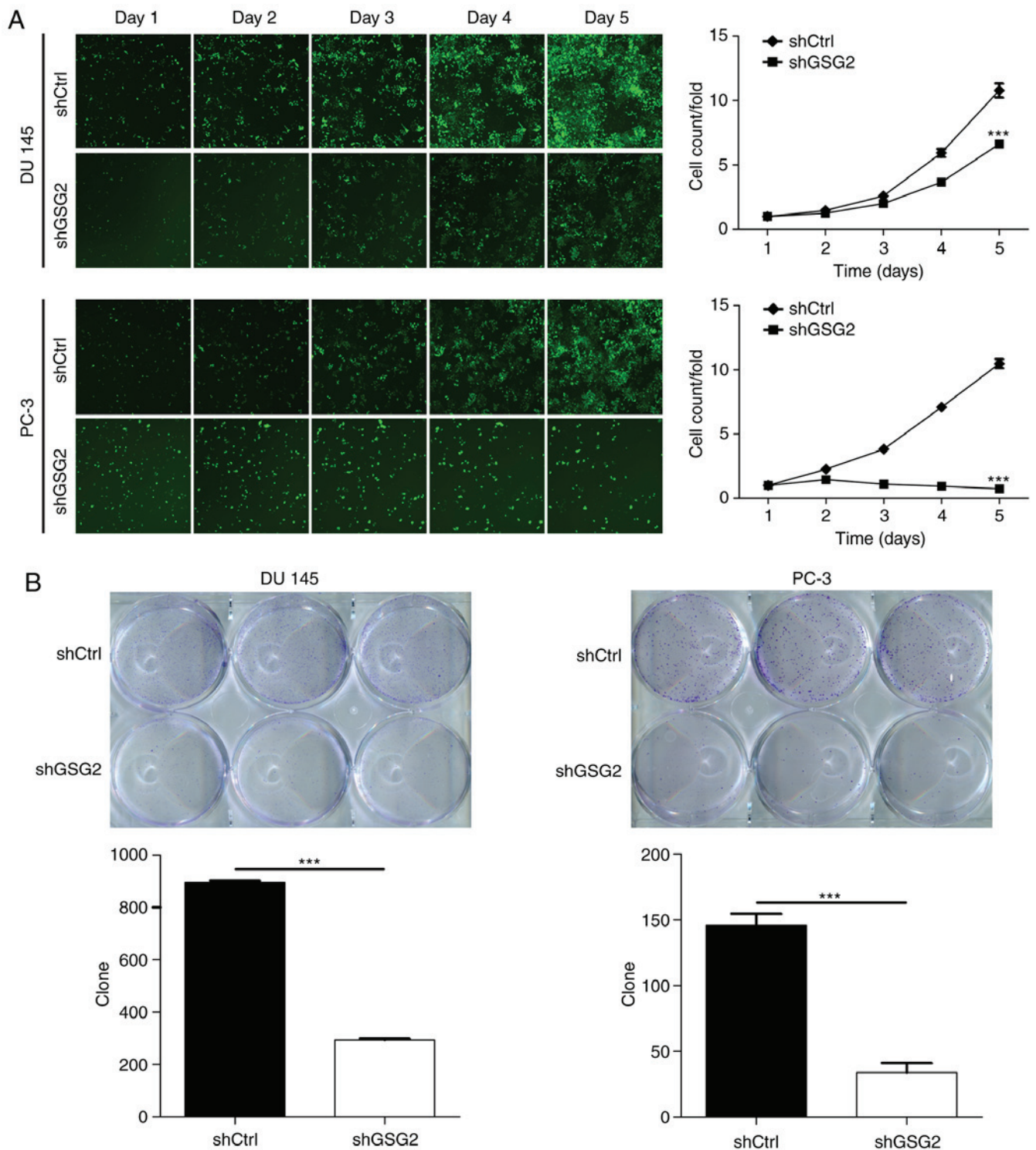
Figure 2. GSG2 knockdown inhibits the proliferation and colony formation of PC-3 and DU 145 cells. (A) The effects of GSG2 knockdown on the viability of PC-3 and DU 145 cells was investigated by the Celigo cell counting assay. Compared with the shCtrl group, the growth rates of DU 145 and PC-3 cells were decreased in the shGSG2 group. (B) Compared with the shCtrl group, the number of colony formation of DU 145 and PC-3 cells was decreased in the shGSG2 group. ***P<0.001. GSG2, germ cell-specific gene 2; shGSG2, cells transfected with GSG2-targeting short hairpin RNA; shCtrl, cells transfected with the control short hairpin RNA.

the proliferation of PCa cells was significantly inhibited in the shGSG2 group compared with that in the shCtrl group (Fig. 4G). These results confirmed that GSG2 knockdown suppressed tumor development *in vivo*. Taken together, these results indicated that targeting GSG2 with shGSG2 may have an inhibitory effect on PCa *in vivo*.

Mechanism of GSG2 knockdown in PC-3 cells. To investigate the regulatory mechanism of GSG2 in the tumor development of PCa, Human RTK Phosphorylation Antibody Array was used in the shGSG2 and shCtrl groups of PC-3 cells for exploring potential downstream signaling pathways and functional targets that mediate the effect of GSG2 knockdown on
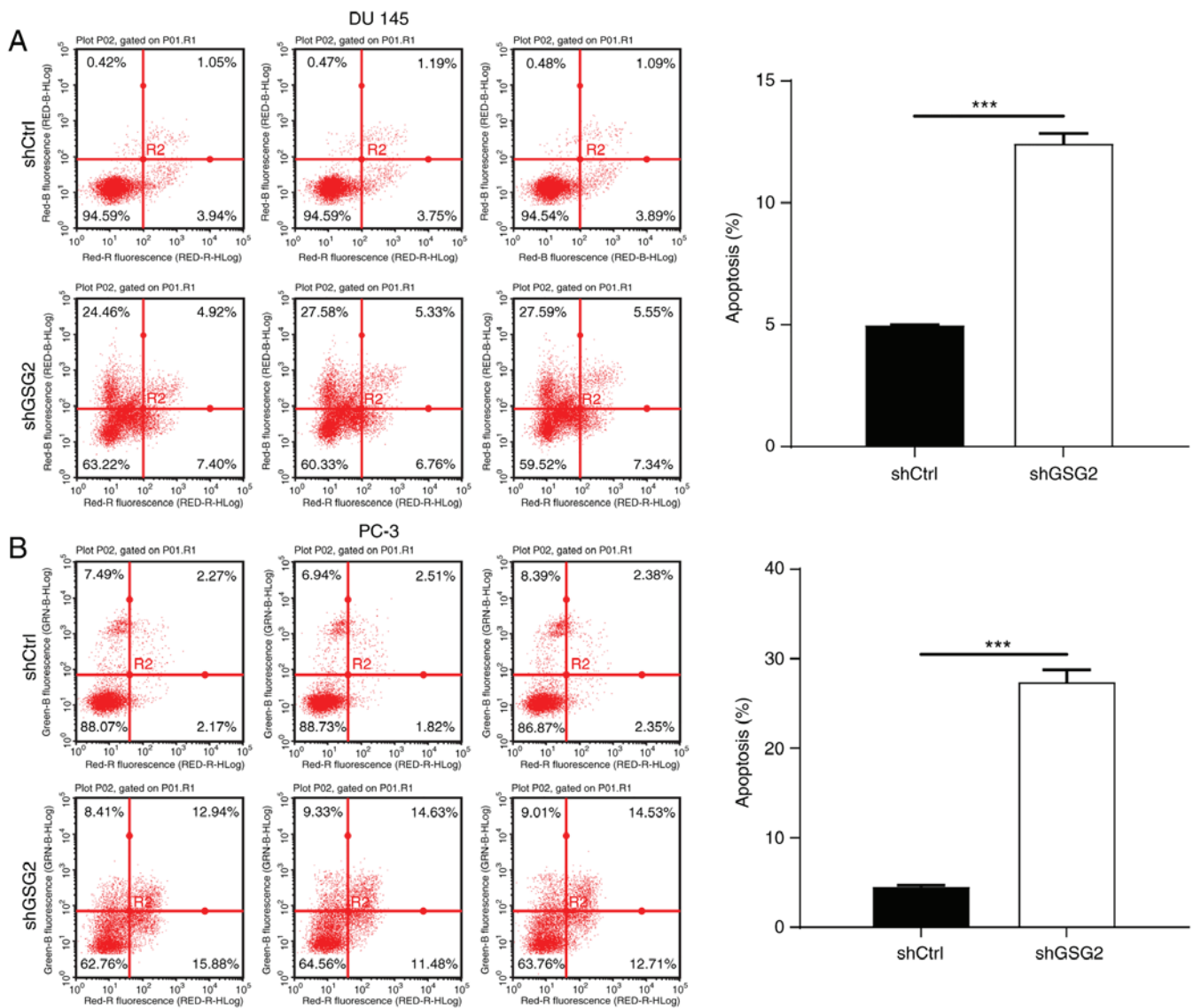
Figure 3. GSG2 knockdown promotes apoptosis of DU 145 and PC-3 cells. (A) The percentage of apoptosis in DU 145 cells was detected by FACS in each group. (B) FACS results in PC-3 cells. The apoptotic rate of PC-3 cells was increased in the shGSG2 group compared with the shCtrl group. ***P<0.001. GSG2, germ cell-specific gene 2; FACS, fluorescence-activated cell sorting; shGSG2, cells transfected with GSG2-targeting short hairpin RNA; shCtrl, cells transfected with the control short hairpin RNA.

PCa. Among them, the levels of ephrin receptor A4 (EphA4), EphA5, EphA6, EphA7, EphB3, FER tyrosine kinase (FER), insulin-like growth factor (IGF)-IR, interleukin-2-inducible T-cell kinase (Itk), Janus kinase 2 (JAK2), JAK3, leukocyte receptor tyrosine kinase (LTK), Lyn proto-oncogene Src family tyrosine kinase (Lyn), macrophage colony-stimulating factor 1 receptor (M-CSFR), muscle-associated receptor tyrosine kinase (MUSK), nerve growth factor receptor (NGFR), platelet-derived growth factor receptor α (PDGFR-α), ROS proto-oncogene 1 receptor tyrosine kinase (ROS), tyrosine-protein kinase Srms (SRMS), TXK tyrosine kinase (TXK), tyrosine kinase 2 (Tyk2) and zeta chain of T-cell receptor-associated protein kinase 70 (ZAP70) were determined to be significantly downregulated in PC-3 cells following GSG2 knockdown compared with cells infected with shCtrl (P<0.05; Fig. 5A-D), indicating the potential functional targets in the regulatory effect of GSG2 on PCa and guiding the direction of our future work.

Discussion

The treatment of PCa has attracted increasing attention in recent years (12). Previous studies have reported numerous gene targets that were able to inhibit cell proliferation and promote apoptosis in PCa (21-23). A recent study has suggested that certain natural products, such as green tea, can effectively induce apoptosis and inhibit invasion of PCa cells via the PI3K/Akt signaling pathway (24). However, more efficient and accurate targets still need to be explored.

The GSG2 kinase is a member of the eukaryotic protein kinase (ePK) family that structurally diverges from the majority of ePKs (25). A number of studies have tried to use small molecule inhibitors to determine the functions of GSG2 in mitosis (26,27); to the best of our knowledge, histone H3 phosphorylated by GSG2 at threonine-3 (H3T3ph) is the only currently known product of GSG2 activity; thus, GSG2 inhibitors strongly reduce the levels of H3T3ph in cells (28).
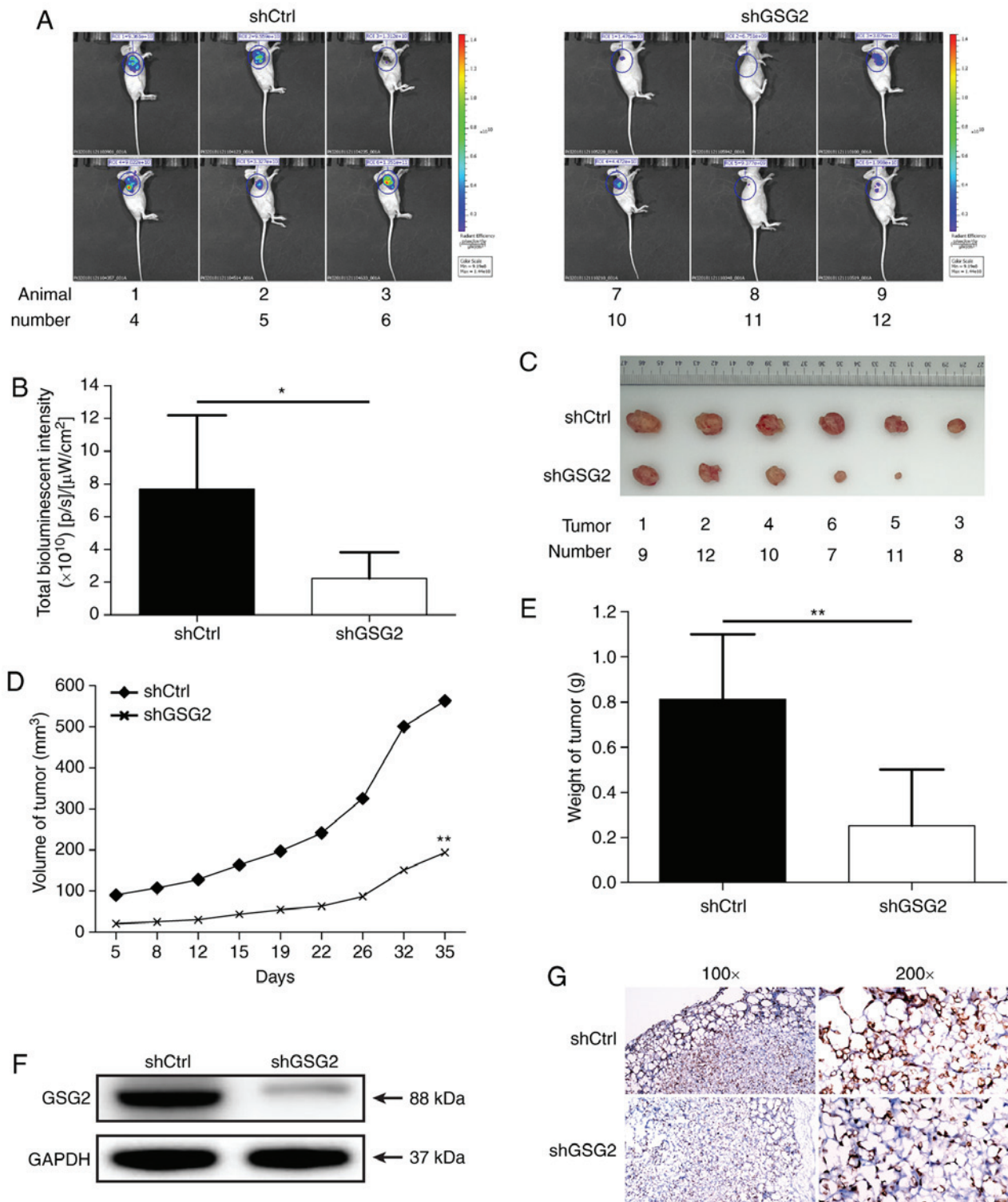
Figure 4. Effects of GSG2 knockdown on tumor progression *in vivo*. (A) The results of in vivo imaging of mouse xenografts. (B) The bioluminescence intensity in shGSG2 group was significantly weaker compared with that in the shCtrl group. (C) Representative images of tumors. (D) Changes in the tumor volume throughout the experiment. (E) Mean tumor weight in the two groups. (F) GSG2 protein levels in tumor tissues from mice were determined by western blotting. (G) Changes in Ki-67 expression in tumors excised from mice (magnification, x100 or x200). *$P<0.05$, **$P< 0.01$. GSG2, germ cell-specific gene 2; shGSG2, mice injected with cells transfected with GSG2-targeting short hairpin RNA; shCtrl, mice injected with cells transfected with the control short hairpin RNA.

However, research on GSG2 in prostate tumors is rare. The present study initially detected GSG2 expression in PCa tissues by immunohistochemical staining, and the results revealed that GSG2 expression levels in PCa tissues were significantly higher compared with those in para-carcinoma tissues. Therefore, to study the role of GSG2 in PCa cells,

PC-3 and DU 145 cells were selected for the construction of GSG2-knockdown cell models.

Kim *et al* (16,29) demonstrated that the inhibition of GSG2 activity by coumestrol inhibited the proliferation of cancer cells. In our study, Celigo cell counting assay was performed to demonstrate the effect of GSG2 knockdown on PCa cell
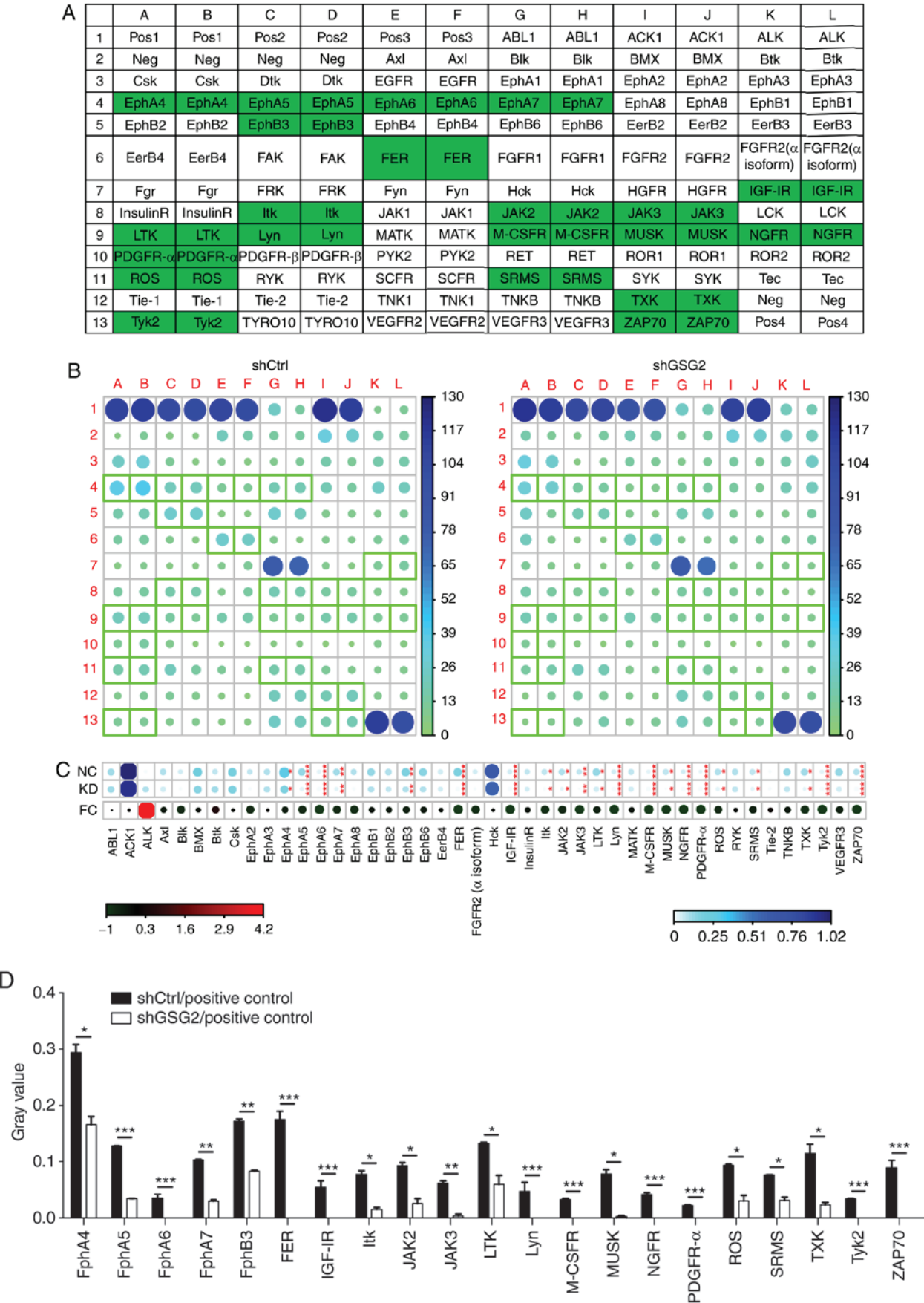
Figure 5. Mechanism of GSG2 silencing in PC-3. (A) Arrangement and distribution of proteins in intracellular signaling array after shGSG2 lentivirus infection. (B) Results of protein expression in the intracellular signaling array after shGSG2 infection. (C) Fold-changes of protein expression in the intracellular signaling array after shGSG2 infection. (D) Plot histogram of GSG2-related signaling molecules in cancer cells by SignaLink 2.0 analysis. *P<0.05, **P<0.01, ***P<0.001. GSG2, germ cell-specific gene 2; shGSG2, cells transfected with GSG2-targeting short hairpin RNA; shCtrl, cells transfected with the control short hairpin RNA.

proliferation, and the results demonstrated that cell proliferation was significantly inhibited in the shGSG2 group compared with that in the shCtrl group, which was consistent with the results of the colony formation assay. The results of the present study also revealed that knockdown of GSG2 increased the apoptotic rate of PC-3 and DU 145 cells. In addition, it was observed that the growth of PCa tumors *in vivo* was significantly inhibited in the shGSG2 group compared with that in the shCtrl group, which was also confirmed by the relatively lower Ki-67 expression in the tumors of the shGSG2 group. The levels of bioluminescence intensity also revealed marked inhibition of tumor growth in the shGSG2 group.

Zabala-Letona *et al* (30) have reported that the production of polyamine is a hallmark of highly proliferating cells, and an essential metabolic route for oncogenicity is mechanistic target of rapamycin complex 1, which regulates polyamine dynamics. The present study preliminarily screened the regulatory mechanism of GSG2 in tumor development in PCa. The results revealed that knockdown of GSG2 inhibited the phosphorylation of EphA4, EphA5, EphA6, EphA7, EphB3, FER, IGF-IR, Itk, JAK2, JAK3, LTK, Lyn, M-CSFR, MUSK, NGFR, PDGFR-α, ROS, SRMS, TXK, Tyk2 and ZAP70 in PCa cells compared with those infected with shCtrl. According to previous studies, EphA4, EphA5, EphA6 and EphA7 promote angiogenesis and PCa metastasis, and are associated with human PCa progression (29,31-33). FER kinase serves a central role in breast cancer metastasis and PCa cell proliferation (34). IGF serves key roles in the progression of different types of cancer, such as breast, prostate, lung, ovarian and skin cancer (35). The JAK2 signaling pathway is involved in cytokine signaling, which regulates hematopoietic cell development, cell metabolism and immune responses (36). In addition, LTK shares a high degree of similarity with anaplastic lymphoma kinase, which is mutated in human cancers including adenocarcinomas of the lung, neuroblastomas, breast and esophageal cancers (37). TXK is a member of the Tec family of tyrosine kinases, which acts as Th1 cell-specific transcription factor (38). These results suggested that GSG2 may serve a crucial role in the establishment and progression of PCa.

The present study had certain limitations, including the low number of clinical specimens. In addition, the specific downstream genes and regulatory mechanisms must be investigated and verified in the future. Further research is needed to discover the prognostic significance of GSG2 in PCa and the role of GSG2 in different PCa cell lines.

In conclusion, the present study is the first to link GSG2 to PCa progression. The results of the present study suggested that GSG2 knockdown inhibited the development and progression of PCa. Thus, GSG2 may be a potential therapeutic target for PCa treatment.

Acknowledgements

Availability of data and materials

The datasets used and/or analyzed during the current study are available from the corresponding author on reasonable request.

Authors' contributions

AX designed the study. FY and YL conceived and coordinated the study, performed experiments, analyzed the data and wrote the manuscript. XX, WL, DT and YZ collected and analyzed the data and revised the manuscript. XZ and GW supervised the study and participated in the writing of the manuscript. All authors reviewed the results and approved the final version of the manuscript.

Ethics approval and consent to participate

Ethical approval was obtained from the Ethics Committee of the First Affiliated Hospital of Nanchang University and informed written consent was obtained from all patients. All animal experiments were approved and performed under the supervision of the Institutional Animal Care and Use Ethics Committee of the First Affiliated Hospital of Nanchang University.

Patient consent for publication

Not applicable.

Competing interests

The authors declare that they have no competing interests.

References

1. Weng CC, Ding PY, Liu YH, Hawse JR, Subramaniam M, Wu CC, Lin YC, Chen CY, Hung WC and Cheng KH: Mutant Kras-induced upregulation of CD24 enhances prostate cancer stemness and bone metastasis. Oncogene 38: 2005-2019, 2019.
2. Rawla P: Epidemiology of prostate cancer. World J Oncol 10: 63-89, 2019.
3. Fong LY, Jing R, Smalley KJ, Wang ZX, Taccioli C, Fan S, Chen H, Alder H, Huebner K, Farber JL, *et al*: Human-like hyperplastic prostate with low ZIP1 induced solely by Zn deficiency in rats. Proc Natl Acad Sci USA 115: E11091-E11100, 2018.
4. Barry MJ and Simmons LH: Prevention of prostate cancer morbidity and mortality: Primary prevention and early detection. Med Clin North Am 101: 787-806, 2017.
5. Daniyal M, Siddiqui ZA, Akram M, Asif HM, Sultana S and Khan A: Epidemiology, etiology, diagnosis and treatment of prostate cancer. Asian Pac J Cancer Prev 15: 9575-9578, 2014.
6. Cuzick J, Thorat MA, Andriole G, Brawley OW, Brown PH, Culig Z, Eeles RA, Ford LG, Hamdy FC, Holmberg L, *et al*: Prevention and early detection of prostate cancer. Lancet Oncol 15: e484-e492, 2014.
7. Pezaro C, Woo HH and Davis ID: Prostate cancer: Measuring PSA. Intern Med J 44: 433-440, 2014.
8. Mohamad NV, Soelaiman IN and Chin KY: A review on the effects of androgen deprivation therapy (ADT) on bone health status in men with prostate cancer. Endocr Metab Immune Disord Drug Targets 17: 276-284, 2017.

9. Munkley J, Vodak D, Livermore KE, James K, Wilson BT, Knight B, Mccullagh P, Mcgrath J, Crundwell M, Harries LW, *et al*: Glycosylation is an androgen-regulated process essential for prostate cancer cell viability. EBioMedicine 8: 103-116, 2016.

10. Reina-Campos M, Linares JF, Duran A, Cordes T, L'Hermitte A, Badur MG, Bhangoo MS, Thorson PK, Richards A, Rooslid T, *et al*: Increased serine and one-carbon pathway metabolism by PKClambda/iota deficiency promotes neuroendocrine prostate cancer. Cancer Cell 35: 385-400.e9, 2019.

11. Xu K, Ganapathy K, Andl T, Wang Z, Copland JA, Chakrabarti R and Florczyk SJ: 3D porous chitosan-alginate scaffold stiffness promotes differential responses in prostate cancer cell lines. Biomaterials 217: 119311, 2019.

12. Dai J, Sultan S, Taylor SS and Higgins JM: The kinase haspin is required for mitotic histone H3 Thr 3 phosphorylation and normal metaphase chromosome alignment. Genes Dev 19: 472-488, 2005.

13. Kestav K, Uri A and Lavogina D: Structure, Roles and inhibitors of a mitotic protein kinase haspin. Curr Med Chem 24: 2276-2293, 2017.

14. Opoku-Temeng C, Dayal N, Aflaki Sooreshjani M and Sintim HO: 3H-pyrazolo[4,3-f]quinoline haspin kinase inhibitors and anticancer properties. Bioorg Chem 78: 418-426, 2018.

15. Lavogina D, Kestav K, Chaikuad A, Heroven C, Knapp S and Uri A: Co-crystal structures of the protein kinase haspin with bisubstrate inhibitors. Acta Crystallogr F Struct Biol Commun 72: 339-345, 2016.

16. Kim JE, Lee SY, Jang M, Choi HK, Kim JH, Chen H, Lim TG, Dong Z and Lee KW: Coumestrol epigenetically suppresses cancer cell proliferation: Coumestrol is a natural haspin kinase inhibitor. Int J Mol Sci 18: pii: E2228, 2017.

17. Amoussou NG, Bigot A, Roussakis C and Robert JH: Haspin: A promising target for the design of inhibitors as potent anticancer drugs. Drug Discov Today 23: 409-415, 2018.

18. Han L, Wang P, Sun Y, Liu S and Dai J: Anti-melanoma activities of haspin inhibitor CHR-6494 deployed as a single agent or in a synergistic combination with MEK inhibitor. J Cancer 8: 2933-2943, 2017.

19. Scheff NN, Alemu RG, Klares R III, Wall IM, Yang SC, Dolan JC and Schmidt BL: Granulocyte-colony stimulating factor-induced neutrophil recruitment provides opioid-mediated endogenous anti-nociception in female mice with oral squamous cell carcinoma. Front Mol Neurosci 12: 217, 2019.

20. Pfaffl MW Pfaffl: A new mathematical model for relative quantification in real-time RT-PCR. Nucleic Acids Res 29: e45, 2001.

21. Metzger E, Wang S, Urban S, Willmann D, Schmidt A, Offermann A, Allen A, Sum M, Obier N, Cottard F, *et al*: KMT9 monomethylates histone H4 lysine 12 and controls proliferation of prostate cancer cells. Nat Struct Mol Biol 26: 361-371, 2019.

22. Fong KW, Zhao JC, Song B, Zheng B and Yu J: TRIM28 protects TRIM24 from SPOP-mediated degradation and promotes prostate cancer progression. Nat Commun 9: 5007, 2018.

23. Canesin G, Evans-Axelsson S, Hellsten R, Sterner O, Krzyzanowska A, Andersson T and Bjartell A: The STAT3 inhibitor galiellalactone effectively reduces tumor growth and metastatic spread in an orthotopic xenograft mouse model of prostate cancer. Eur Urol 69: 400-404, 2016.

24. Wang Z, Wang Y, Zhu S, Liu Y, Peng X, Zhang S, Zhang Z, Qiu Y, Jin M, Wang R, *et al*: DT-13 inhibits proliferation and metastasis of human prostate cancer cells through blocking PI3K/Akt pathway. Front Pharmacol 9: 1450, 2018.

25. Maiolica A, de Medina-Redondo M, Schoof EM, Chaikuad A, Villa F, Gatti M, Jeganathan S, Lou HJ, Novy K, Hauri S, *et al*: Modulation of the chromatin phosphoproteome by the Haspin protein kinase. Mol Cell Proteomics 13: 1724-1740, 2014.

26. Patnaik D, Jun X, Glicksman MA, Cuny GD, Stein RL and Higgins JM: Identification of small molecule inhibitors of the mitotic kinase haspin by high-throughput screening using a homogeneous time-resolved fluorescence resonance energy transfer assay. J Biomol Screen 13: 1025-1034, 2008.

27. Balzano D, Santaguida S, Musacchio A and Villa F: A general framework for inhibitor resistance in protein kinases. Chem Biol 18: 966-975, 2011.

28. Wang F, Ulyanova NP, Daum JR, Patnaik D, Kateneva AV, Gorbsky GJ and Higgins JM: Haspin inhibitors reveal centromeric functions of Aurora B in chromosome segregation. J Cell Biol 199: 251-268, 2012.

29. Li S, Wu Z, Ma P, Xu Y, Chen Y, Wang H, He P, Kang Z, Yin L, Zhao Y, *et al*: Ligand-dependent EphA7 signaling inhibits prostate tumor growth and progression. Cell Death Dis 8: e3122, 2017.

30. Zabala-Letona A, Arruabarrena-Aristorena A, Martín-Martín N, Fernandez-Ruiz S, Sutherland JD, Clasquin M, Tomas-Cortazar J, Jimenez J, Torres I, Quang P, *et al*: mTORC1-dependent AMD1 regulation sustains polyamine metabolism in prostate cancer. Nature 547: 109-113, 2017.

31. Jing X, Sonoki T, Miyajima M, Sawada T, Terada N, Takemura S and Sakaguchi K: EphA4-deleted microenvironment regulates cancer development and leukemoid reaction of the isografted 4T1 murine breast cancer via reduction of an IGF1 signal. Cancer Med 5: 1214-1227, 2016.

32. Li S, Zhu Y, Ma C, Qiu Z, Zhang X, Kang Z, Wu Z, Wang H, Xu X, Zhang H, *et al*: Downregulation of EphA5 by promoter methylation in human prostate cancer. BMC Cancer 15: 18, 2015.

33. Li S, Ma Y, Xie C, Wu Z, Kang Z, Fang Z, Su B and Guan M: EphA6 promotes angiogenesis and prostate cancer metastasis and is associated with human prostate cancer progression. Oncotarget 6: 22587-22597, 2015.

34. Ivanova IA, Vermeulen JF, Ercan C, Houthuijzen JM, Saig FA, Vlug EJ, van der Wall E, van Diest PJ, Vooijs M and Derksen PW: FER kinase promotes breast cancer metastasis by regulating α6- and β1-integrin-dependent cell adhesion and anoikis resistance. Oncogene 32: 5582-5592, 2013.

35. Vishwamitra D, George SK, Shi P, Kaseb AO and Amin HM: Type I insulin-like growth factor receptor signaling in hematological malignancies. Oncotarget 8: 1814-1844, 2017.

36. Jay J, Hammer A, Nestor-Kalinoski A and Diakonova M: JAK2 tyrosine kinase phosphorylates and is negatively regulated by centrosomal protein Ninein. Mol Cell Biol 35: 111-131, 2015.

37. Roll JD and Reuther GW: ALK-activating homologous mutations in LTK induce cellular transformation. PLoS One 7: e31733, 2012.

38. Prchal-Murphy M, Witalisz-Siepracka A, Bednarik KT, Putz EM, Gotthardt D, Meissl K, Sexl V, Müller M and Strobl B: In vivo tumor surveillance by NK cells requires TYK2 but not TYK2 kinase activity. Oncoimmunology 4: e1047579, 2015.